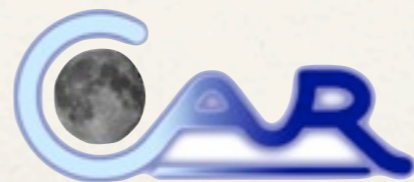




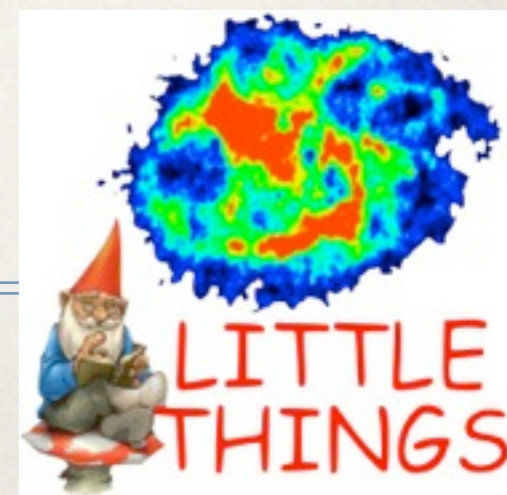
Phases of the ISM as seen by LITTLE THINGS

Elias Brinks
Centre for Astrophysics Research
University of Hertfordshire



Date: 1st August 2013

Phases of the ISM, Heidelberg



Content

- ❖ Brief overview of LITTLE THINGS
- ❖ Breaking the metallicity barrier: CO in the dIrr galaxy WLM

Content

- ❖ Brief overview of LITTLE THINGS
- ❖ Breaking the metallicity barrier: CO in the dwarf galaxy WLM

Yeah!!!

LITTLE THINGS

LITTLE: Local Irregulars That Trace Luminosity Extremes

THINGS: The HI Nearby Galaxy Survey

DDO 75



Messier 74 = NGC 628

LITTLE THINGS provides observations of the neutral, atomic gas phase with the Karl G. Jansky VLA, the reservoir of the fuel for star formation



The Team

Deidre Hunter (PI, Lowell Observatory)
Elias Brinks (Univ of Hertfordshire, UK)
Bruce Elmegreen (IBM T. J. Watson Research Center)
Michael Rupen (NRAO)
Caroline Simpson (Florida International Univ)
Fabian Walter (MPIA, Germany)
David Westpfahl (New Mexico Tech)
Lisa Young (New Mexico Tech)

Trisha Ashley (pre-doc, FIU)
Phil Cigan (pre-doc, New Mexico Tech)
Dana Ficut-Vicas (pre-doc, Univ Hertfordshire)
Ged Kitchener (pre-doc, Univ Hertfordshire)
Volker Heesen (post-doc, Univ Southampton)
Kim Herrmann (Penn State – Mont Alto)
Megan Jackson (post-doc NRAO)
Se-Heon Oh (Univ Western Australia)
Andreas Schruba (CalTech)
Hongxin Zhang (Peking Univ)



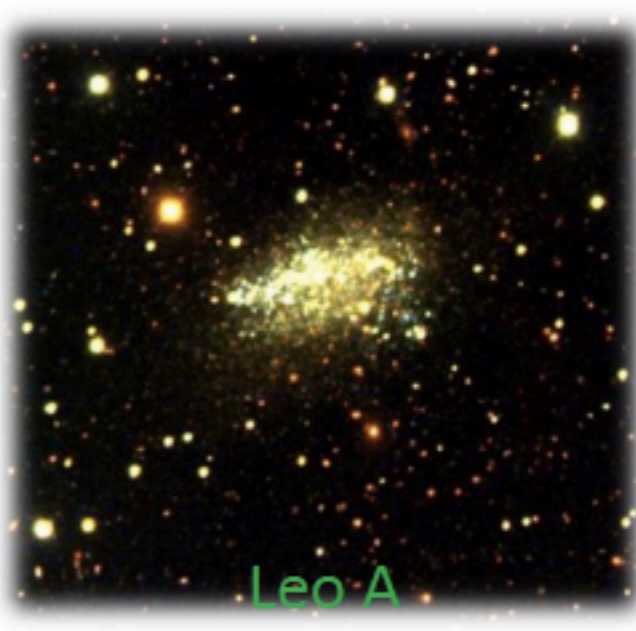
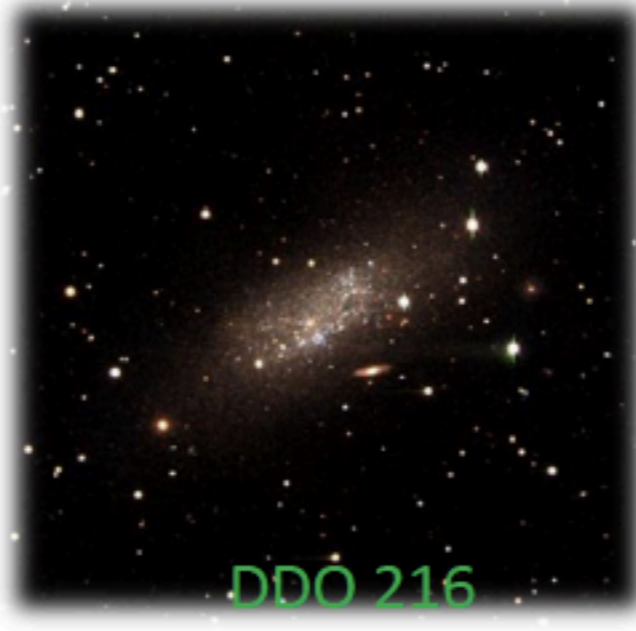
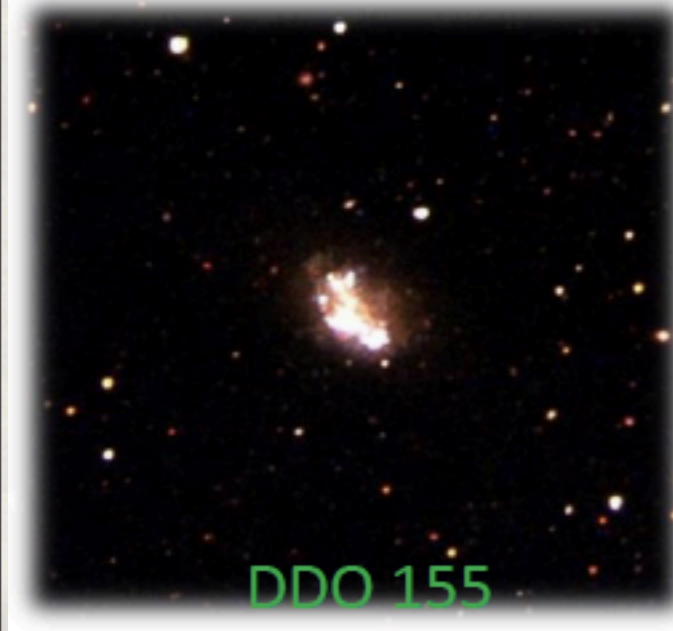
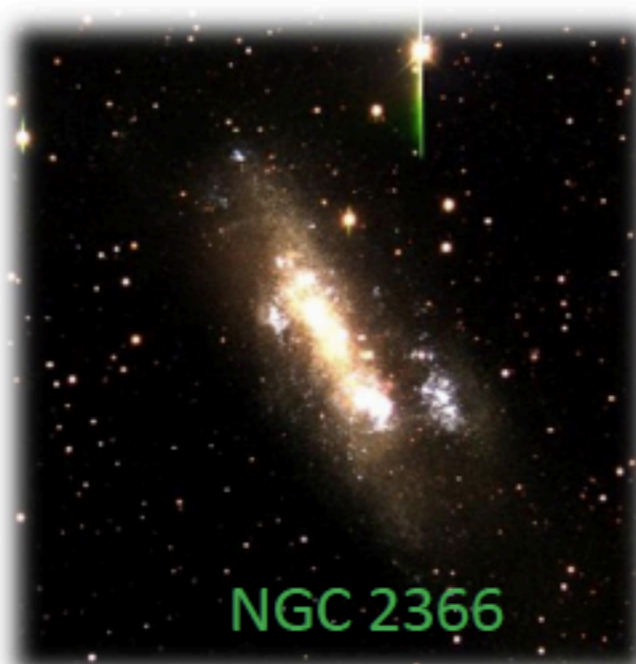
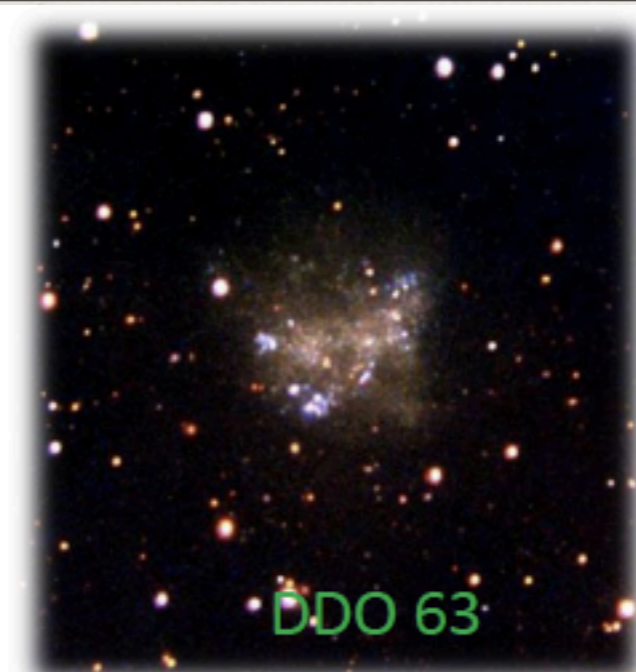
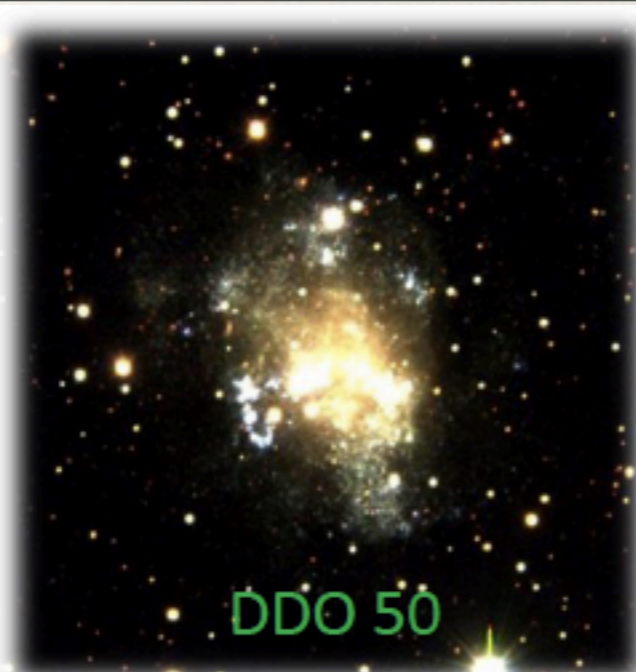
LT Team meeting, Lowell Observatory, June 2012

The Sample

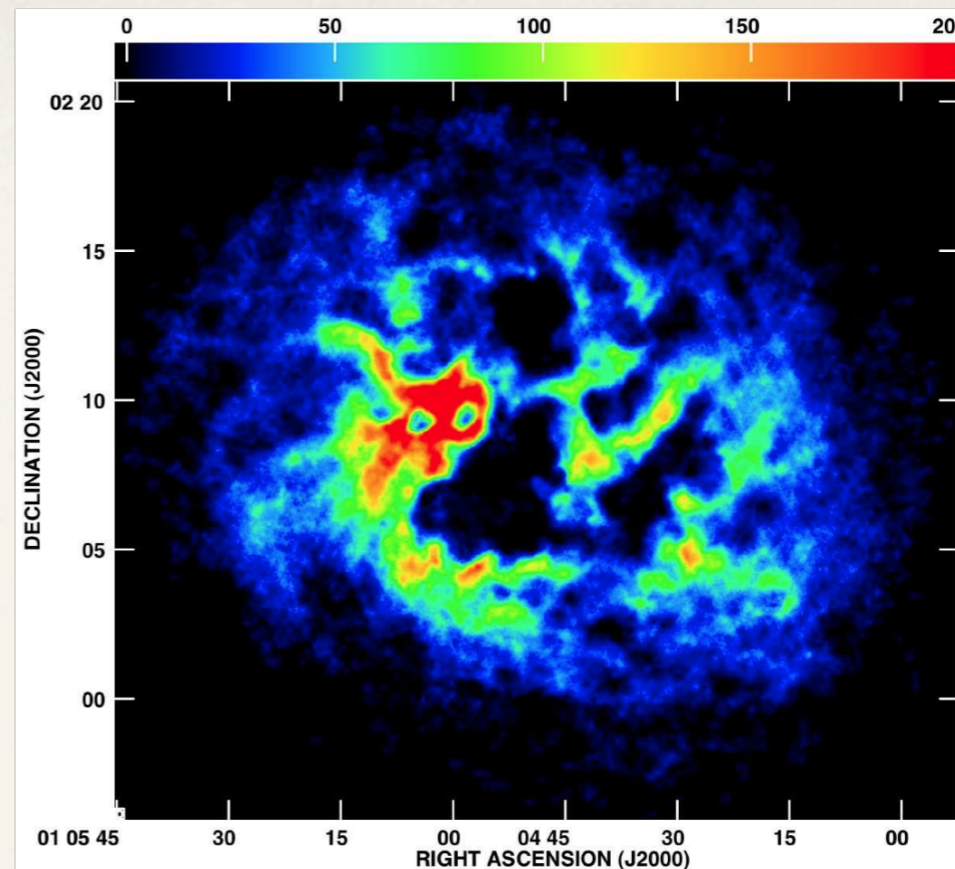
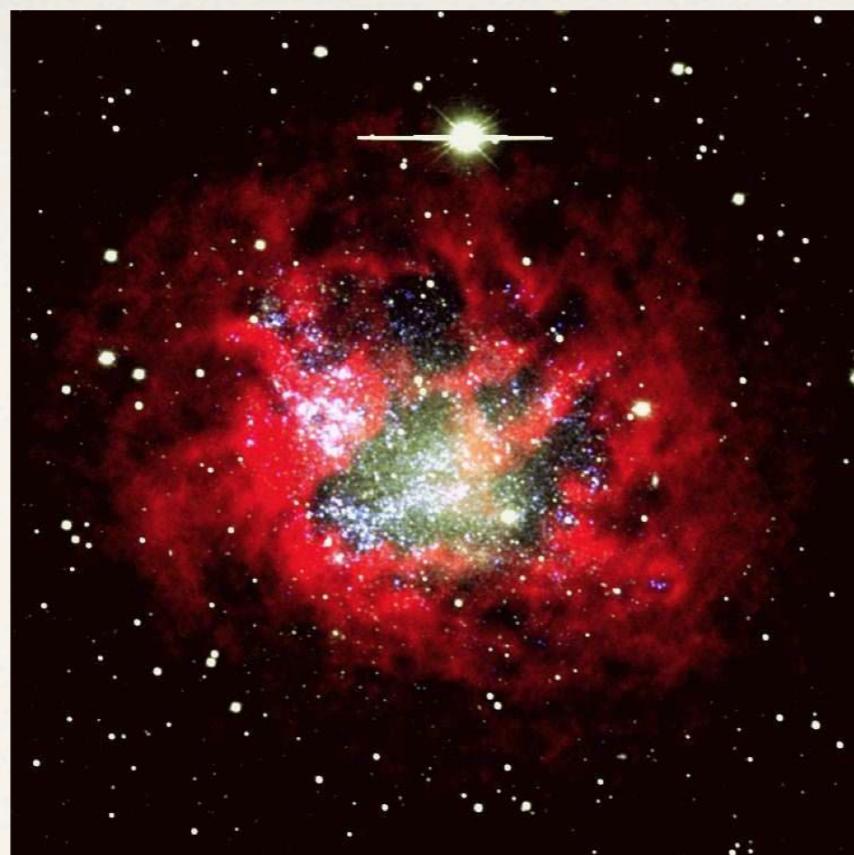
The larger sample was selected to have gas, so targets could form stars in principle, and not be obviously interacting as we are interested in internal triggering processes (Hunter & Elmegreen 2004, 2006).

The LITTLE THINGS sub-sample, 42 targets, covers the range of properties of the larger survey; it is representative and includes the extremes.

Galaxy	VLA Array		Ch sep (km/s)	D (Mpc)	M_V (mag)	R_H^a (arcmin)	Incl. (deg)	$\log M_{HI}$ (M_\odot)	$\log \text{SFR}_D^b$ ($M_\odot / \text{yr} / \text{kpc}^2$)
	Archive	New Obs							
Im Galaxies									
CVnIdwA	C	BD	1.3	4.1	-12.6	0.87	40	7.79	-2.64
DDO 43	CD	B	2.6	5.5	-14.3	0.89	48	7.97	-2.19
DDO 46		BCD	2.6	5.5	-14.4	9.99	28	8.13	-2.96
DDO 47	BCD		2.6	5.2	-15.5	2.24	64	8.60	-2.75
DDO 50	BCD		2.6	3.4	-16.6	3.97	46	8.86	-1.83
DDO 52		BCD	2.6	6.0	-14.3	1.08	51	7.97	-3.27
DDO 53	BCD		2.6	3.6	-13.8	1.37	64	8.26	-2.50
DDO 63	BCD		2.6	3.8	-14.7	2.17	0	8.18	-3.44
DDO 69	BCD		1.3	0.8	-11.7	2.40	60	7.00	-3.28
DDO 70	BCD		1.3	1.3	-14.1	3.71	57	7.59	-2.86
DDO 75	BCD		2.6	1.3	-13.9	3.09	33	7.88	-1.40
DDO 87	C	BD	2.6	6.7	-14.7	1.15	58	8.24	-3.16
DDO 101	C	BD	2.6	9.0	-15.8	1.05	49	7.27	-2.99
DDO 126		BCD	1.3	4.9	-14.8	1.76	67	8.14	-2.45
DDO 133	D	BC	2.6	6.1	-16.0	2.33	49	8.58	-2.93
DDO 154	BCD		2.6	4.3	-14.5	1.55	65	8.49	-2.60
DDO 155	C	BD	1.3	2.2	-12.5	0.95	47	7.00	-1.50
DDO 165		BCD	1.3	4.8	-15.7	2.14	61	8.19	-3.52
DDO 167		BCD	1.3	4.2	-13.0	0.75	52	7.26	-2.41
DDO 168		BCD	2.6	3.5	-15.3	2.32	54	8.35	-2.33
DDO 187		BCD	1.3	2.5	-13.0	1.06	38	7.35	-2.64
DDO 210	BCD		1.3	0.9	-10.9	1.31	66	6.39	0
DDO 216	CD		1.3	0.9	-13.3	4.00	69	5.89	-4.15
F564-V3	CD	B	1.3	6.2	-13.2	9.99	35	7.14	0
IC 10	ABC		2.6	1.0	-17.1	9.99	40	8.34	-1.31
IC 1613	BCD		2.6	0.7	-14.6	9.10	37	7.53	-2.64
LGS 3	CD		1.3	0.6	-9.4	0.96	64	5.05	0
M81dwA	BCD		1.3	3.6	-11.7	9.99	45	7.13	0
NGC 1156	BCD		1.3	7.8	-18.7	2.14	32	9.03	-0.87
NGC 1569	BCD		2.6	2.5	-17.6	9.99	61	7.99	0.11
NGC 2366	BCD		2.6	3.2	-16.7	4.72	72	8.83	-1.73
NGC 3738		BCD	2.6	4.9	-17.1	2.40	0	8.19	-1.72
NGC 4163	D	BC	2.6	2.8	-14.4	1.47	53	7.18	-2.43
NGC 4214	BCD		1.3	2.9	-17.6	4.67	25	8.75	-1.10
NGC 6822		BCD	1.3	0.5	-15.2	9.99	40	8.11	-1.96
SagDIG	CD		1.3	1.1	-12.4	9.99	62	6.90	-3.02
UGC 8508		BCD	1.3	2.6	-13.6	1.28	61	7.41	-2.12
WLM	BCD		2.6	1.0	-14.4	5.81	70	7.77	-2.85
BCD Galaxies									
Haro 29		BCD	1.3	5.4	-14.5	0.84	58	7.80	-0.82
Haro 36		BCD	2.6	9.0	-15.8	9.99	37	8.16	-1.96
Mrk 178		BCD	1.3	3.9	-14.1	1.01	68	7.00	-1.53
VII Zw 403	BCD		2.6	4.4	-14.3	1.11	66	7.85	-1.82

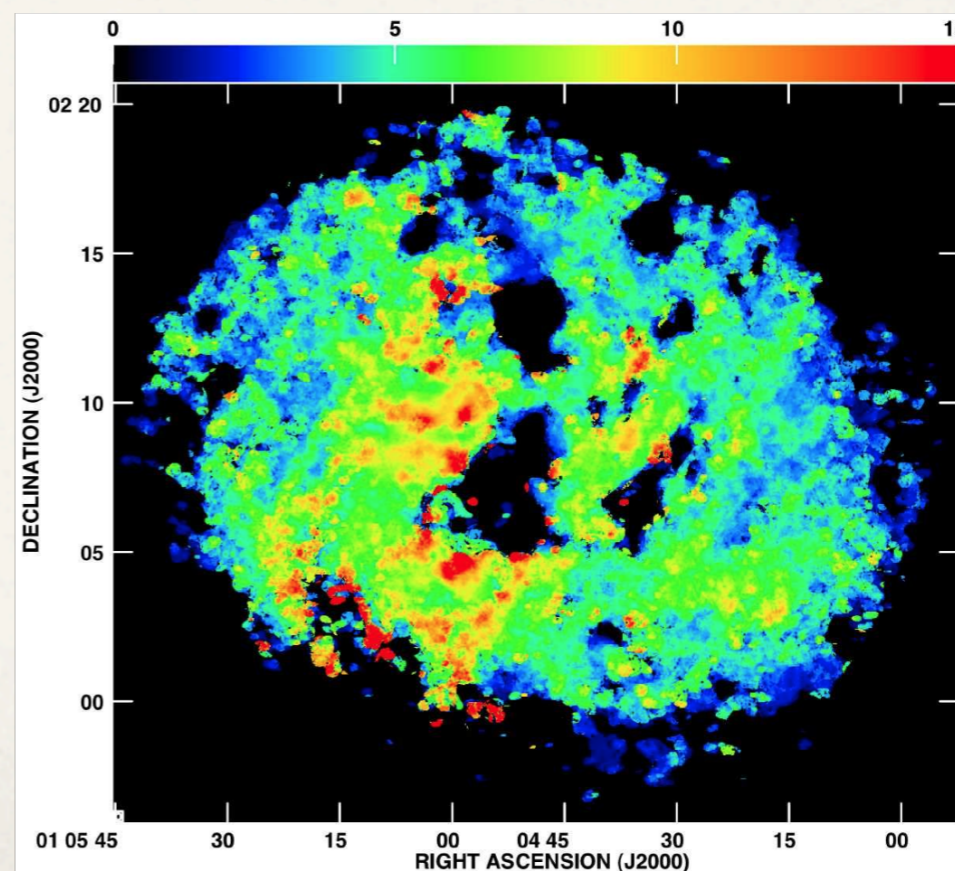
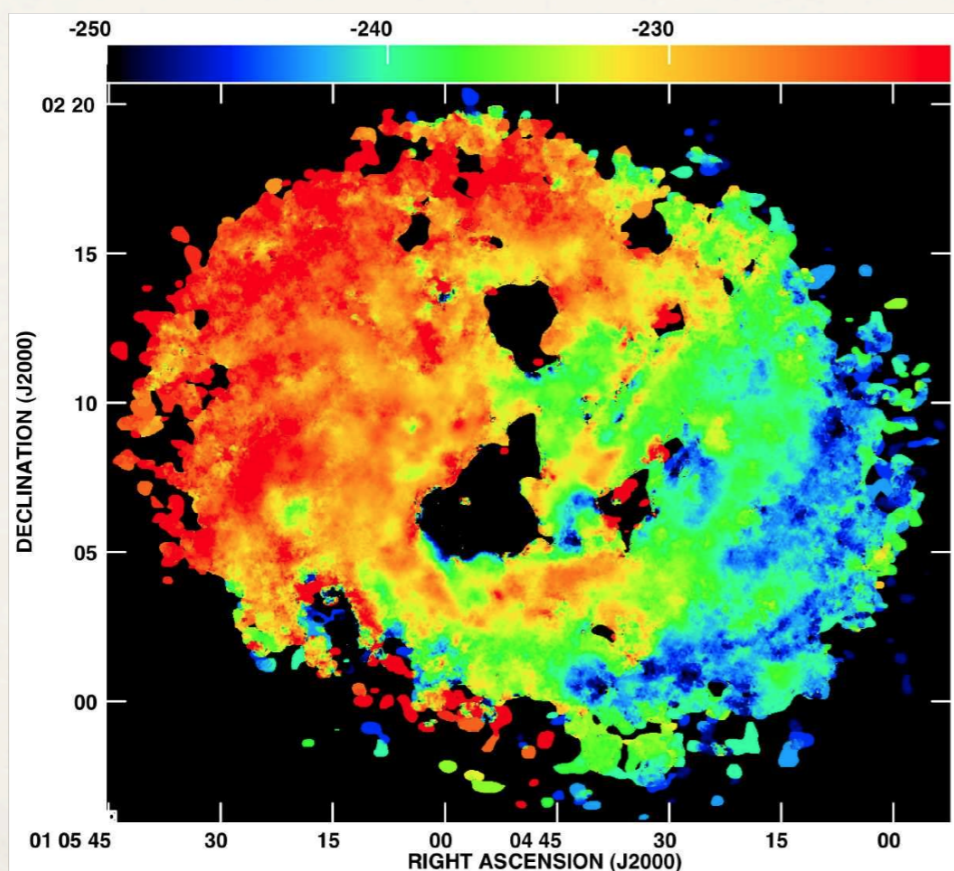


IC 1613



HI

HI on
optical/UV



σ

V_{hel}

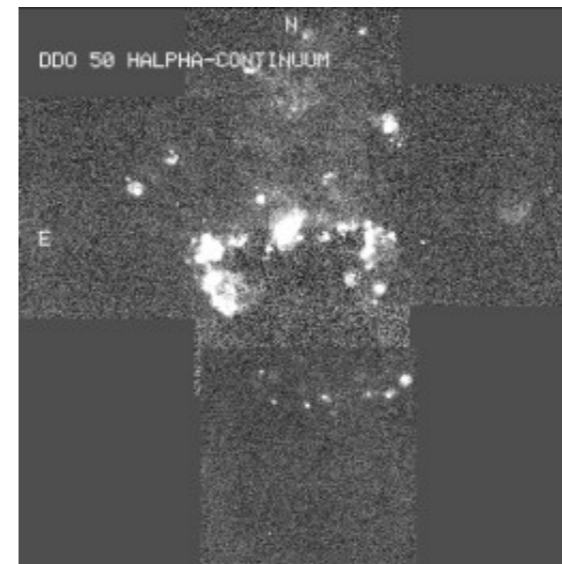
DDO 50 metadata

DDO 50 metadata

- VLA HI: Observations
- *UBV* images
 - FITS files: *U, B, V*
 - Calibration parameters
 - Further information: Hunter & Elmegreen 2006
- *JHK* images: None
- Halpha images
 - FITS files:
 - Halpha (with stars)
 - Halpha (minus stellar continuum and sky)
 - Calibration parameters
 - Further information: Hunter & Elmegreen 2004
- Ultraviolet images
 - FITS files: FUV, NUV
 - Further information: Hunter, Elmegreen, & Ludka 2010, Zhang et al. (2011)
- *Spitzer* IRAC images
 - FITS files: LVL IRAC Data
 - Further information: Hunter, Elmegreen, & Martin 2006



<https://science.nrao.edu/science/surveys/littlethings/>



DDO 50 metadata

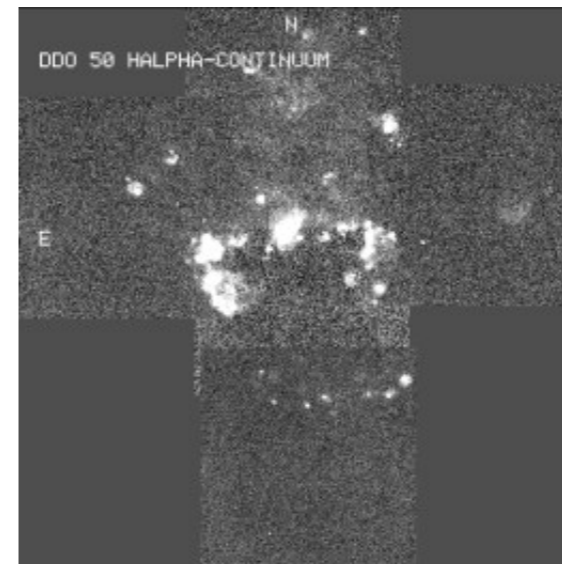
NEW: 6cm radio continuum survey

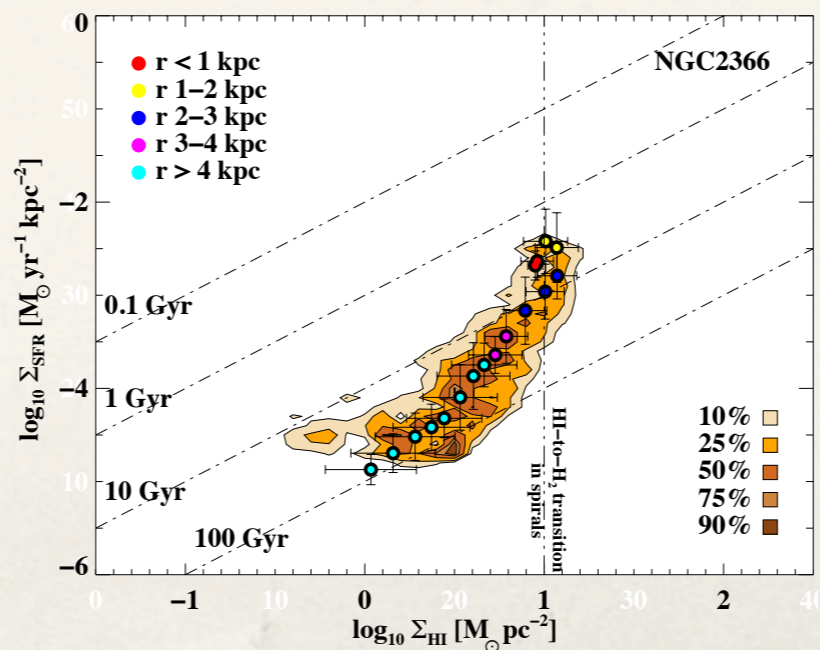
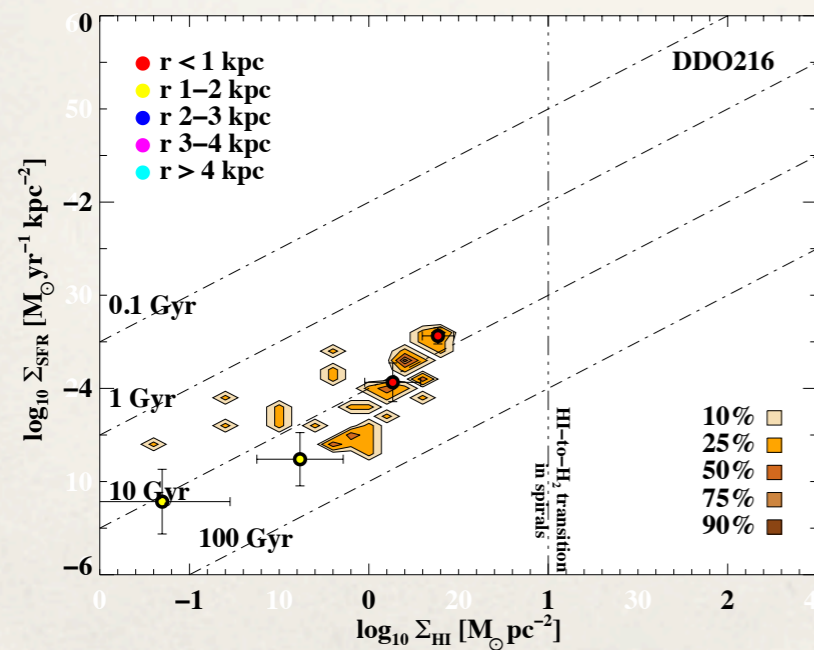
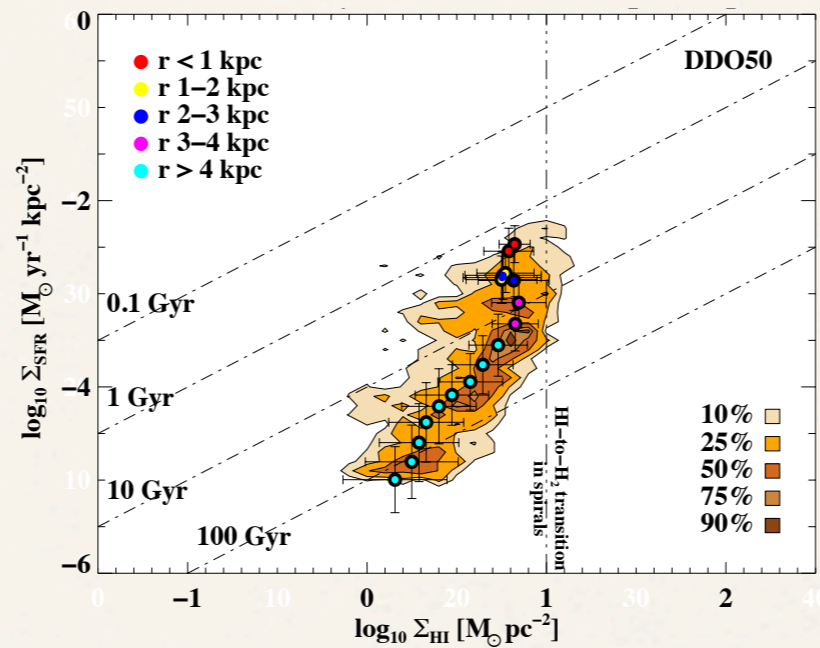
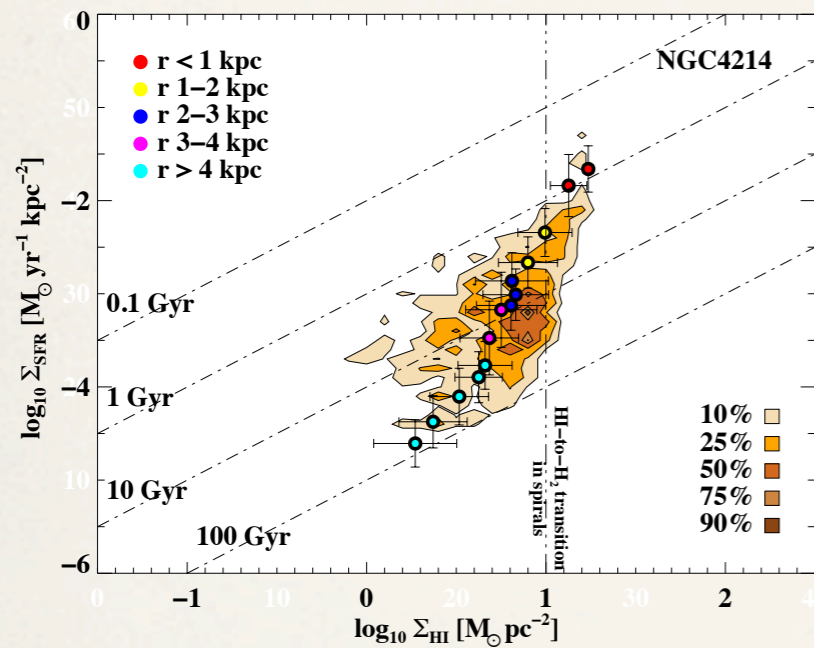
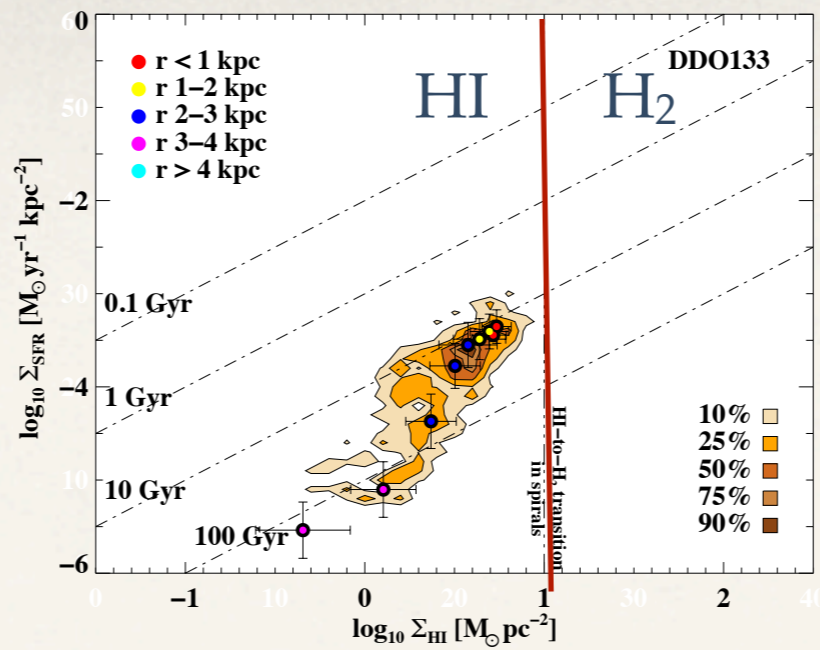
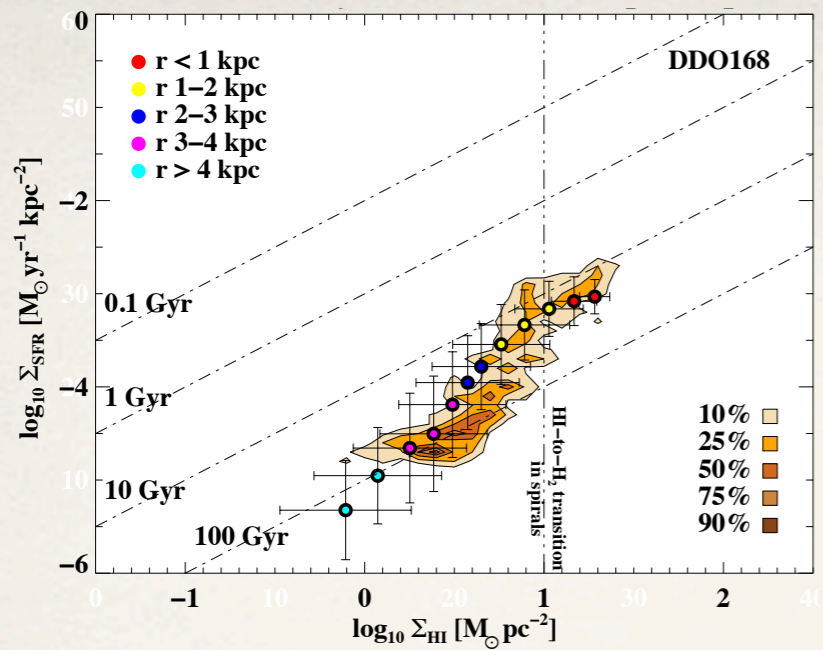
DDO 50 metadata

- VLA HI: Observations
- *UBV* images
 - FITS files: *U, B, V*
 - Calibration parameters
 - Further information: Hunter & Elmegreen 2006
- *JHK* images: None
- Halpha images
 - FITS files:
 - Halpha (with stars)
 - Halpha (minus stellar continuum and sky)
 - Calibration parameters
 - Further information: Hunter & Elmegreen 2004
- Ultraviolet images
 - FITS files: FUV, NUV
 - Further information: Hunter, Elmegreen, & Ludka 2010, Zhang et al. (2011)
- *Spitzer* IRAC images
 - FITS files: LVL IRAC Data
 - Further information: Hunter, Elmegreen, & Martin 2006



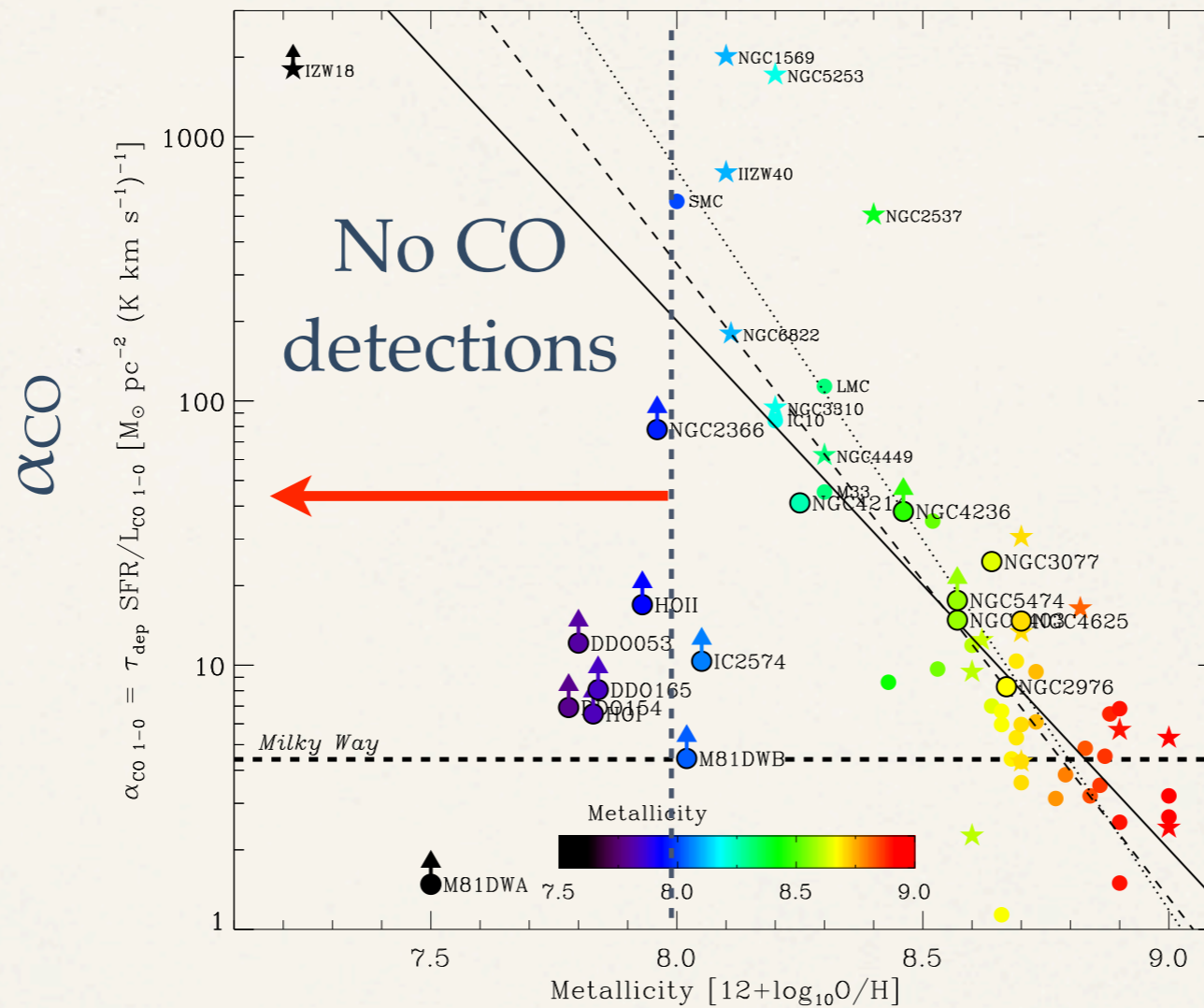
<https://science.nrao.edu/science/surveys/littlethings/>





SK-plots for some of the LT dwarfs: SFR density versus HI surface density. Coloured symbols are radial averages. Cell size: 400 pc.

X-factor - metallicity relation



metallicity

Carbon monoxide in clouds at low metallicity in the dwarf irregular galaxy WLM

Bruce G. Elmegreen¹, Monica Rubio², Deldre A. Hunter³, Celia Verdugo², Elias Brinks⁴ & Andreas Schruba⁵

Carbon monoxide (CO) is the primary tracer for interstellar clouds where stars form, but it has never been detected in galaxies in which the oxygen abundance relative to hydrogen is less than 20 per cent of that of the Sun, even though such 'low-metallicity' galaxies often form stars. This raises the question of whether stars can form in dense gas without molecules, cooling to the required near-zero temperatures by atomic transitions and dust radiation rather than by molecular line emission¹; and it highlights uncertainties about star formation in the early Universe, when the metallicity was generally low. Here we report the detection of CO in two regions of a local dwarf irregular galaxy, WLM, where the metallicity is 13 per cent of the solar value^{2,3}. We use new submillimetre observations and archival far-infrared observations to estimate the cloud masses, which are both slightly greater than 100,000 solar masses. The clouds have produced stars at a rate per molecule equal to 10 per cent of that in the local Orion nebula cloud. The CO fraction of the molecular gas is also low, about 3 per cent of the Milky Way value. These results suggest that in small galaxies both star-forming cores and CO molecules become increasingly rare in molecular hydrogen clouds as the metallicity decreases.

Wolf-Lundmark-Melotte (WLM) is an isolated dwarf galaxy at the edge of the Local Group⁴. It has a low star-formation rate because of its small size and, like other dwarf irregular (dIrr) galaxies, shows no previous evidence⁵ for the molecular gas that always accompanies young stars in larger galaxies⁶. One problem with the detection of molecules is that the dominant tracer of such gas is CO, and dIrr galaxies have low carbon and oxygen abundances relative to hydrogen. No galaxy with an O/H abundance less than 20% has been detected using CO as a tracer⁷⁻⁹. Far more abundant is molecular hydrogen (H₂), but this does not have an observable state of excitation at the low temperatures (~10–30 K) required for star formation.

To search for star-forming gas, we surveyed WLM for CO(*J* = 3–2) emission in rotational state *J* and for continuum dust emission at 345 GHz using the Atacama Pathfinder Experiment (APEX) telescope at Llano de Chajnantor, Chile, with the Swedish Heterodyne Facility Instrument¹⁰ and the Large APEX Bolometer Camera¹¹ (LABOCA). We also used a map of dust emission at 160 μm from the Spitzer Local Volume Legacy Survey¹² and a map of atomic hydrogen re-reduced from the archives of the Jansky Very Large Array radio telescope. The

dust measurements can be converted to a dust temperature and a dust mass, and, after applying a suitable gas-to-dust ratio, to a gas mass from which the H I mass can be subtracted to give the H₂ mass for comparison with CO.

Figure 1 shows WLM and the two regions, designated A and B, where we detected CO(3–2) emission, along with H I, far-infrared (FIR) and submillimetre images. Observed and derived parameters are listed in Tables 1 and 2, respectively. The peak CO brightness temperature in each detected region is ~0.01–0.015 K and the line-width is ~12 km s⁻¹ (full-width at half-maximum). Previous efforts to detect CO(*J* = 1–0) in WLM⁵ partly overlapped region A with a 45'' aperture and determined a 5σ upper limit to the CO(1–0) intensity of 0.18 K km s⁻¹. Our observation with an 18'' aperture yields an intensity of 0.200 ± 0.046 K km s⁻¹ for CO(3–2) in the same region. The difference arises because the CO cloud is unresolved even by our 18'' beam—we did not detect comparable CO(3–2) intensities in our searches adjacent to region A. The previous upper limit corresponds to a maximum CO(1–0) luminosity of 8,300 K km s⁻¹ pc² inside 45'' (which corresponds to a beam diameter of 215 pc at WLM), whereas the cloud we detect has a CO(3–2) luminosity ~6 times smaller (1,500 K km s⁻¹ pc²). Likewise, the previous null detection⁵ in CO(*J* = 2–1) claimed a 5σ upper limit that is about the same as our CO(3–2) detection, but their closest pointing differed from region A by ~70 pc (14'', or half the beam diameter for CO(2–1)), which could have been enough to take it off the CO cloud.

The 160-μm, 870-μm and H I peaks are slightly offset from the CO positions, indicating variations in temperature and molecular fraction. A large H I and FIR cloud that surrounds region A, designated region A1, was used to measure the dust temperature, *T*_d ~ 15 K, which was assumed to be the same throughout the region (the 160-μm observation does not resolve region A, and so a more localized temperature measurement is not possible). We determined *T*_d from the 870-μm and 160-μm fluxes corrected for the CO(3–2) line and broadband free-free emission (Table 1), assuming a modified black-body function with dust emissivity proportional to frequency to the power β. Local measurements¹³ suggest that β = 1.78 ± 0.08, although a range is possible^{14,15}, depending on grain temperature and properties¹⁶. The 870-μm flux was also corrected for an unexplained FIR and submillimetre excess that is commonly observed in other low-metallicity galaxies^{17,18}. An alternate

Table 1 | Observations of WLM

Source	Region	Right ascension	Declination	Beam diameter (")	Flux
CO(3–2)	A	0 h 1 min 57.32 s	–15° 26' 49.5''	18	0.200 ± 0.046 K km s ⁻¹
H I	A	0 h 1 min 57.32 s	–15° 26' 49.5''	22	774 ± 40 mJy km s ⁻¹
870 μm	A	0 h 1 min 57.32 s	–15° 26' 49.5''	22	2.66 ± 0.53 mJy (0.11, 0.02)*
H I	A1	0 h 1 min 56.93 s	–15° 26' 40.84''	45	4.170 ± 82 mJy km s ⁻¹
870 μm	A1	0 h 1 min 56.93 s	–15° 26' 40.84''	45	15.2 ± 3.0 mJy (0.11, 0.06)*
160 μm	A1	0 h 1 min 56.93 s	–15° 26' 40.84''	45	136.2 ± 13.6 mJy (0.05)†
CO(3–2)	B	0 h 2 min 1.68 s	–15° 27' 52.5''	18	0.129 ± 0.032 K km s ⁻¹

* Quantities in parentheses are the CO(3–2) flux and the free-free emission, both in mJy, that were subtracted from the source flux before calculating the dust flux.

† Quantity in parentheses is the free-free emission, in mJy, that was subtracted from the source flux before calculating the dust flux. The average FIR excess factor¹⁴ for the Small Magellanic Cloud (SMC) is 1.7, so we divide the CO-corrected and free-free-corrected 870-μm fluxes in the table by 1.7 to get the thermal dust flux.

Carbon monoxide in clouds at low metallicity in the dwarf irregular galaxy WLM

Bruce G. Elmegreen¹, Monica Rubio², Deldre A. Hunter³, Celia Verdugo², Elias Brinks⁴ & Andreas Schruba⁵

Breaking the metallicity barrier!!!

Carbon monoxide (CO) is the primary tracer for interstellar clouds where stars form, but it has never been detected in galaxies in which the oxygen abundance relative to hydrogen is less than 20 per cent of that of the Sun, even though such 'low-metallicity' galaxies often form stars. This raises the question of whether stars can form in dense gas without molecules, cooling to the required near-zero temperatures by atomic transitions and dust radiation rather than by molecular line emission¹; and it highlights uncertainties about star formation in the early Universe, when the metallicity was generally low. Here we report the detection of CO in two regions of a local dwarf irregular galaxy, WLM, where the metallicity is 13 per cent of the solar value^{2,3}. We use new submillimetre observations and archival far-infrared observations to estimate the cloud masses, which are both slightly greater than 100,000 solar masses. The clouds have produced stars at a rate per molecule equal to 10 per cent of that in the local Orion nebula cloud. The CO fraction of the molecular gas is also low, about 3 per cent of the Milky Way value. These results suggest that in small galaxies both star-forming cores and CO molecules become increasingly rare in molecular hydrogen clouds as the metallicity decreases.

Wolf-Lundmark-Melotte (WLM) is an isolated dwarf galaxy at the edge of the Local Group⁴. It has a low star-formation rate because of its small size and, like other dwarf irregular (dIrr) galaxies, shows no previous evidence⁵ for the molecular gas that always accompanies young stars in larger galaxies⁶. One problem with the detection of molecules is that the dominant tracer of such gas is CO, and dIrr galaxies have low carbon and oxygen abundances relative to hydrogen. No galaxy with an O/H abundance less than 20% has been detected using CO as a tracer⁷⁻⁹. Far more abundant is molecular hydrogen (H₂), but this does not have an observable state of excitation at the low temperatures (~10–30 K) required for star formation.

To search for star-forming gas, we surveyed WLM for CO(*J* = 3–2) emission in rotational state *J* and for continuum dust emission at 345 GHz using the Atacama Pathfinder Experiment (APEX) telescope at Llano de Chajnantor, Chile, with the Swedish Heterodyne Facility Instrument¹⁰ and the Large APEX Bolometer Camera¹¹ (LABOCA). We also used a map of dust emission at 160 μm from the Spitzer Local Volume Legacy Survey¹² and a map of atomic hydrogen re-reduced from the archives of the Jansky Very Large Array radio telescope. The

dust measurements can be converted to a dust temperature and a dust mass, and, after applying a suitable gas-to-dust ratio, to a gas mass from which the H I mass can be subtracted to give the H₂ mass for comparison with CO.

Figure 1 shows WLM and the two regions, designated A and B, where we detected CO(3–2) emission, along with H I, far-infrared (FIR) and submillimetre images. Observed and derived parameters are listed in Tables 1 and 2, respectively. The peak CO brightness temperature in each detected region is ~0.01–0.015 K and the line-width is ~12 km s⁻¹ (full-width at half-maximum). Previous efforts to detect CO(*J* = 1–0) in WLM⁵ partly overlapped region A with a 45'' aperture and determined a 5σ upper limit to the CO(1–0) intensity of 0.18 K km s⁻¹. Our observation with an 18'' aperture yields an intensity of 0.200 ± 0.046 K km s⁻¹ for CO(3–2) in the same region. The difference arises because the CO cloud is unresolved even by our 18'' beam—we did not detect comparable CO(3–2) intensities in our searches adjacent to region A. The previous upper limit corresponds to a maximum CO(1–0) luminosity of 8,300 K km s⁻¹ pc² inside 45'' (which corresponds to a beam diameter of 215 pc at WLM), whereas the cloud we detect has a CO(3–2) luminosity ~6 times smaller (1,500 K km s⁻¹ pc²). Likewise, the previous null detection⁵ in CO(*J* = 2–1) claimed a 5σ upper limit that is about the same as our CO(3–2) detection, but their closest pointing differed from region A by ~70 pc (14'', or half the beam diameter for CO(2–1)), which could have been enough to take it off the CO cloud.

The 160-μm, 870-μm and H I peaks are slightly offset from the CO positions, indicating variations in temperature and molecular fraction. A large H I and FIR cloud that surrounds region A, designated region A1, was used to measure the dust temperature, *T*_d ~ 15 K, which was assumed to be the same throughout the region (the 160-μm observation does not resolve region A, and so a more localized temperature measurement is not possible). We determined *T*_d from the 870-μm and 160-μm fluxes corrected for the CO(3–2) line and broadband free-free emission (Table 1), assuming a modified black-body function with dust emissivity proportional to frequency to the power β. Local measurements¹³ suggest that β = 1.78 ± 0.08, although a range is possible^{14,15}, depending on grain temperature and properties¹⁶. The 870-μm flux was also corrected for an unexplained FIR and submillimetre excess that is commonly observed in other low-metallicity galaxies^{17,18}. An alternate

Table 1 | Observations of WLM

Source	Region	Right ascension	Declination	Beam diameter (")	Flux
CO(3–2)	A	0 h 1 min 57.32 s	–15° 26' 49.5''	18	0.200 ± 0.046 K km s ⁻¹
H I	A	0 h 1 min 57.32 s	–15° 26' 49.5''	22	774 ± 40 mJy km s ⁻¹
870 μm	A	0 h 1 min 57.32 s	–15° 26' 49.5''	22	2.66 ± 0.53 mJy (0.11, 0.02)*
H I	A1	0 h 1 min 56.93 s	–15° 26' 40.84''	45	4,170 ± 82 mJy km s ⁻¹
870 μm	A1	0 h 1 min 56.93 s	–15° 26' 40.84''	45	15.2 ± 3.0 mJy (0.11, 0.06)*
160 μm	A1	0 h 1 min 56.93 s	–15° 26' 40.84''	45	136.2 ± 13.6 mJy (0.05)†
CO(3–2)	B	0 h 2 min 1.68 s	–15° 27' 52.5''	18	0.129 ± 0.032 K km s ⁻¹

* Quantities in parentheses are the CO(3–2) flux and the free-free emission, both in mJy, that were subtracted from the source flux before calculating the dust flux.

† Quantity in parentheses is the free-free emission, in mJy, that was subtracted from the source flux before calculating the dust flux. The average FIR excess factor¹⁴ for the Small Magellanic Cloud (SMC) is 1.7, so we divide the CO-corrected and free-free-corrected 870-μm fluxes in the table by 1.7 to get the thermal dust flux.

Carbon monoxide in clouds at low metallicity in the dwarf irregular galaxy WLM

Bruce G. Elmegreen¹, Monica Rubio², Deidre A. Hunter³, Celia Verdugo², Elias Brinks⁴ & Andreas Schruba⁵

Carbon monoxide (CO) is the primary tracer for interstellar clouds where stars form, but it has never been detected in galaxies in which the oxygen abundance relative to hydrogen is less than 20 per cent of that of the Sun, even though such 'low-metallicity' galaxies often form stars. This raises the question of whether stars can form in dense gas without molecules, cooling to the required near-zero temperatures by atomic transitions and dust radiation rather than by molecular line emission¹; and it highlights uncertainties about star formation in the early Universe, when the metallicity was generally low. Here we report the detection of CO in two regions of a local dwarf irregular galaxy, WLM, where the metallicity is 13 per cent of the solar value^{2,3}. We use new submillimetre observations and archival far-infrared observations to estimate the cloud masses, which are both slightly greater than 100,000 solar masses. The clouds have produced stars at a rate per molecule equal to 10 per cent of that in the local Orion nebula cloud. The CO fraction of the molecular gas is also low, about 3 per cent of the Milky Way value. These results suggest that in small galaxies both star-forming cores and CO molecules become increasingly rare in molecular hydrogen clouds as the metallicity decreases.

Wolf-Lundmark-Melotte (WLM) is an isolated dwarf galaxy at the edge of the Local Group⁴. It has a low star-formation rate because of its small size and, like other dwarf irregular (dIrr) galaxies, shows no previous evidence⁵ for the molecular gas that always accompanies young stars in larger galaxies⁶. One problem with the detection of molecules is that the dominant tracer of such gas is CO, and dIrr galaxies have low carbon and oxygen abundances relative to hydrogen. No galaxy with an O/H abundance less than 20% has been detected using CO as a tracer⁷⁻⁹. Far more abundant is molecular hydrogen (H₂), but this does not have an observable state of excitation at the low temperatures (~10–30 K) required for star formation.

To search for star-forming gas, we surveyed WLM for CO(*J* = 3–2) emission in rotational state *J* and for continuum dust emission at 345 GHz using the Atacama Pathfinder Experiment (APEX) telescope at Llano de Chajnantor, Chile, with the Swedish Heterodyne Facility Instrument¹⁰ and the Large APEX Bolometer Camera¹¹ (LABOCA). We also used a map of dust emission at 160 μm from the Spitzer Local Volume Legacy Survey¹² and a map of atomic hydrogen re-reduced from the archives of the Jansky Very Large Array radio telescope. The

dust measurements can be converted to a dust temperature and a dust mass, and, after applying a suitable gas-to-dust ratio, to a gas mass from which the H I mass can be subtracted to give the H₂ mass for comparison with CO.

Figure 1 shows WLM and the two regions, designated A and B, where we detected CO(3–2) emission, along with H I, far-infrared (FIR) and submillimetre images. Observed and derived parameters are listed in Tables 1 and 2, respectively. The peak CO brightness temperature in each detected region is ~0.01–0.015 K and the line-width is ~12 km s⁻¹ (full-width at half-maximum). Previous efforts to detect CO(*J* = 1–0) in WLM⁵ partly overlapped region A with a 45'' aperture and determined a 5σ upper limit to the CO(1–0) intensity of 0.18 K km s⁻¹. Our observation with an 18'' aperture yields an intensity of 0.200 ± 0.046 K km s⁻¹ for CO(3–2) in the same region. The difference arises because the CO cloud is unresolved even by our 18'' beam—we did not detect comparable CO(3–2) intensities in our searches adjacent to region A. The previous upper limit corresponds to a maximum CO(1–0) luminosity of 8,300 K km s⁻¹ pc² inside 45'' (which corresponds to a beam diameter of 215 pc at WLM), whereas the cloud we detect has a CO(3–2) luminosity ~6 times smaller (1,500 K km s⁻¹ pc²). Likewise, the previous null detection⁵ in CO(*J* = 2–1) claimed a 5σ upper limit that is about the same as our CO(3–2) detection, but their closest pointing differed from region A by ~70 pc (14'', or half the beam diameter for CO(2–1)), which could have been enough to take it off the CO cloud.

The 160-μm, 870-μm and H I peaks are slightly offset from the CO positions, indicating variations in temperature and molecular fraction. A large H I and FIR cloud that surrounds region A, designated region A1, was used to measure the dust temperature, *T*_d ~ 15 K, which was assumed to be the same throughout the region (the 160-μm observation does not resolve region A, and so a more localized temperature measurement is not possible). We determined *T*_d from the 870-μm and 160-μm fluxes corrected for the CO(3–2) line and broadband free-free emission (Table 1), assuming a modified black-body function with dust emissivity proportional to frequency to the power β. Local measurements¹³ suggest that β = 1.78 ± 0.08, although a range is possible^{14,15}, depending on grain temperature and properties¹⁶. The 870-μm flux was also corrected for an unexplained FIR and submillimetre excess that is commonly observed in other low-metallicity galaxies^{17,18}. An alternate

Table 1 | Observations of WLM

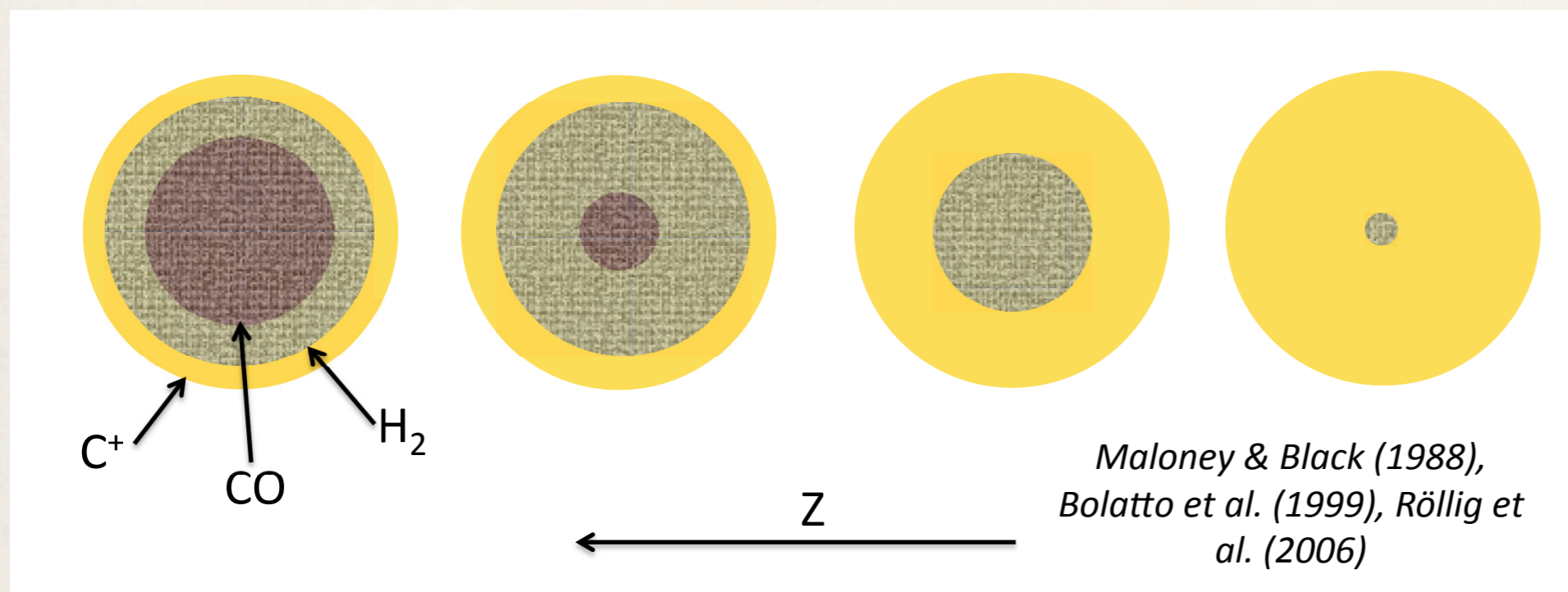
Source	Region	Right ascension	Declination	Beam diameter (")	Flux
CO(3–2)	A	0 h 1 min 57.32 s	–15° 26' 49.5''	18	0.200 ± 0.046 K km s ⁻¹
H I	A	0 h 1 min 57.32 s	–15° 26' 49.5''	22	774 ± 40 mJy km s ⁻¹
870 μm	A	0 h 1 min 57.32 s	–15° 26' 49.5''	22	2.66 ± 0.53 mJy (0.11, 0.02)*
H I	A1	0 h 1 min 56.93 s	–15° 26' 40.84''	45	4,170 ± 82 mJy km s ⁻¹
870 μm	A1	0 h 1 min 56.93 s	–15° 26' 40.84''	45	15.2 ± 3.0 mJy (0.11, 0.06)*
160 μm	A1	0 h 1 min 56.93 s	–15° 26' 40.84''	45	136.2 ± 13.6 mJy (0.05)†
CO(3–2)	B	0 h 2 min 1.68 s	–15° 27' 52.5''	18	0.129 ± 0.032 K km s ⁻¹

* Quantities in parentheses are the CO(3–2) flux and the free-free emission, both in mJy, that were subtracted from the source flux before calculating the dust flux.

† Quantity in parentheses is the free-free emission, in mJy, that was subtracted from the source flux before calculating the dust flux. The average FIR excess factor¹⁴ for the Small Magellanic Cloud (SMC) is 1.7, so we divide the CO-corrected and free-free-corrected 870-μm fluxes in the table by 1.7 to get the thermal dust flux.

Elmegreen et al. 2013,
Nature, 495, 487

GMC as function of Z



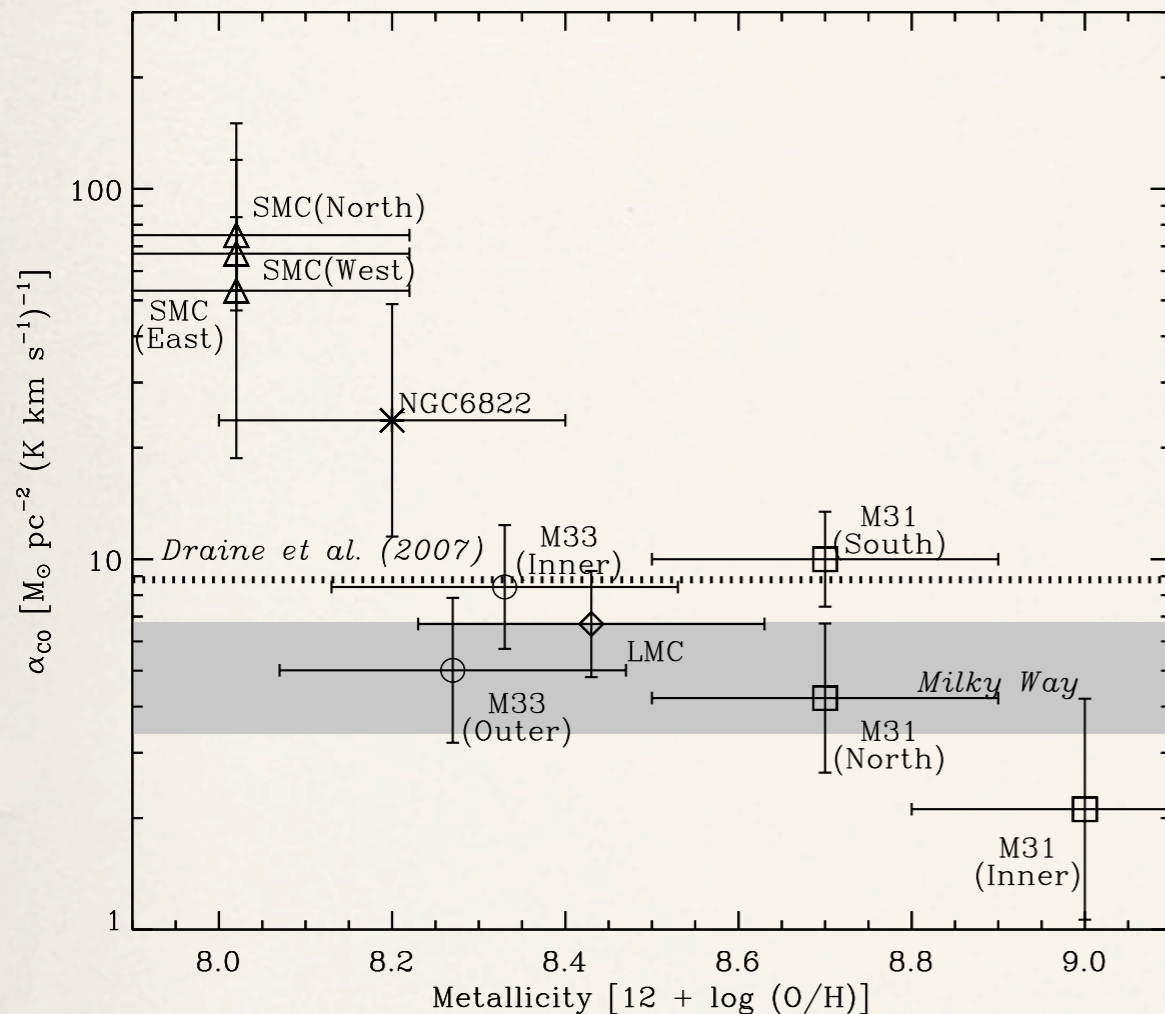
Changing structure of a GMC as metallicity decreases: ISM⁺ (yellow) and PDR (grey) increase while CO (dark grey) decreases. As dust decreases, $A_V \sim 1$ moves deeper into the GMC.

CO disappears $A_V \approx 2$; H₂ can exist at lower A_V .

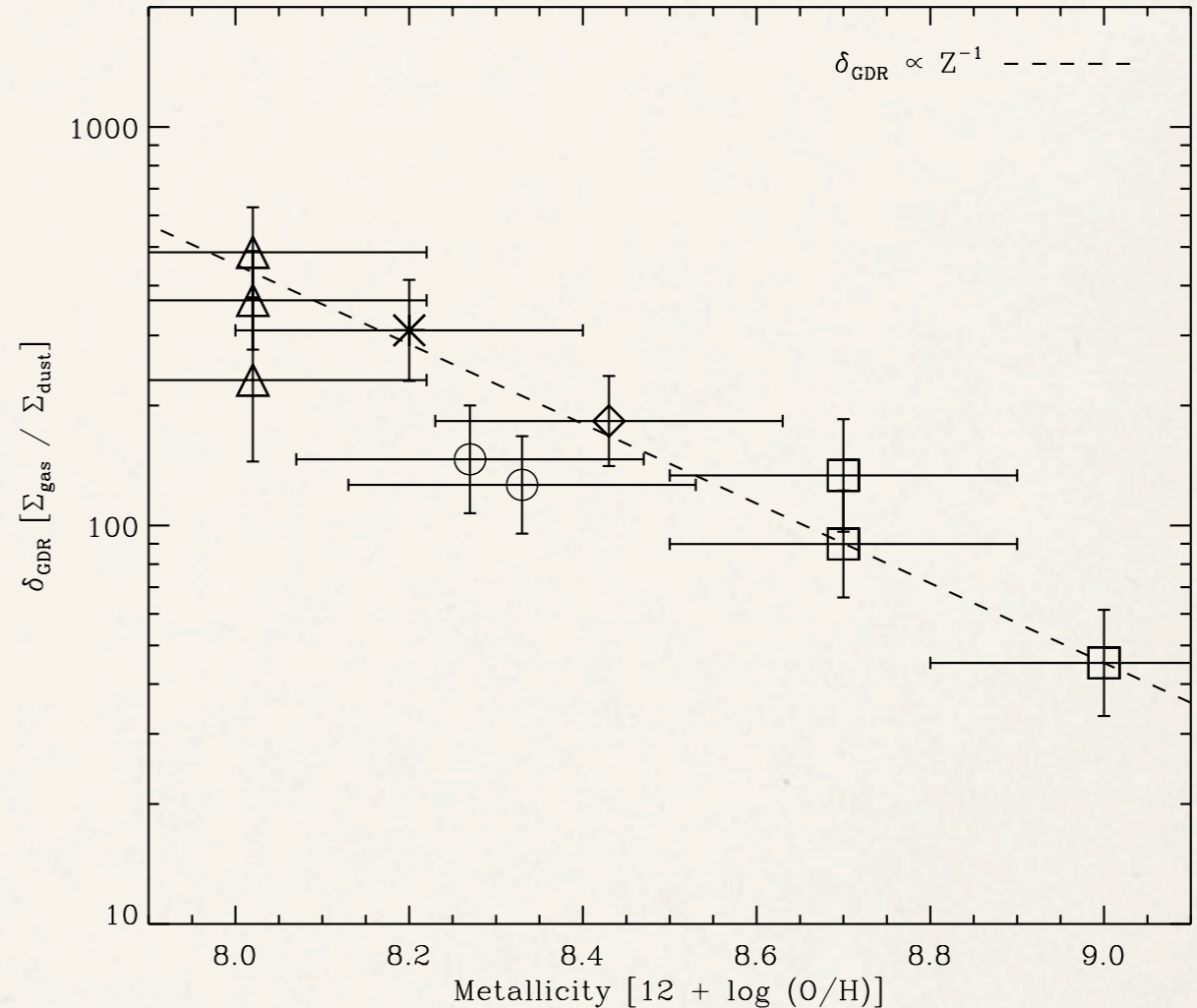
ISM at low metallicity

- ❖ low metallicity \rightarrow low dust content ($GDR \propto Z^{-1}$)
- ❖ PAH emission down
- ❖ T_{dust} increases (~ 32 K in dIrr versus 20-25 K for spirals)
- ❖ excess sub-mm emission beyond $500 \mu\text{m}$ (cold dust reservoir?)
- ❖ [CII] $158 \mu\text{m}$ / CO increases
- ❖ α_{CO} increases steeply with decreasing metallicity

X-factor(Z) and DGR(Z)



α_{CO} increases non-linearly with decreasing metallicity



GDR increases linearly with decreasing metallicity

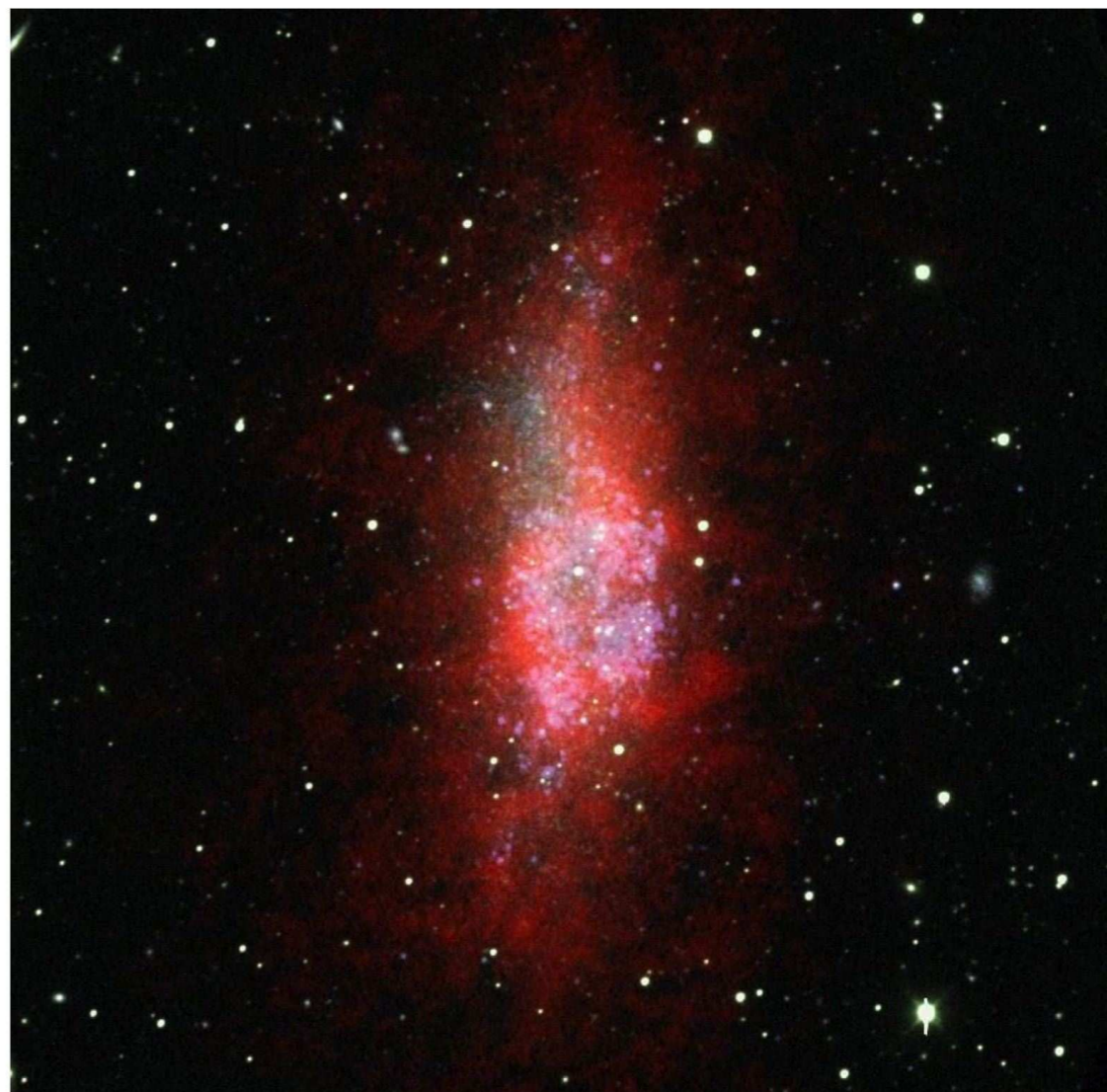
Leroy et al. 2011, ApJ 737, 12

see also Sandstrom et al. 2012, arXiv1212.1208

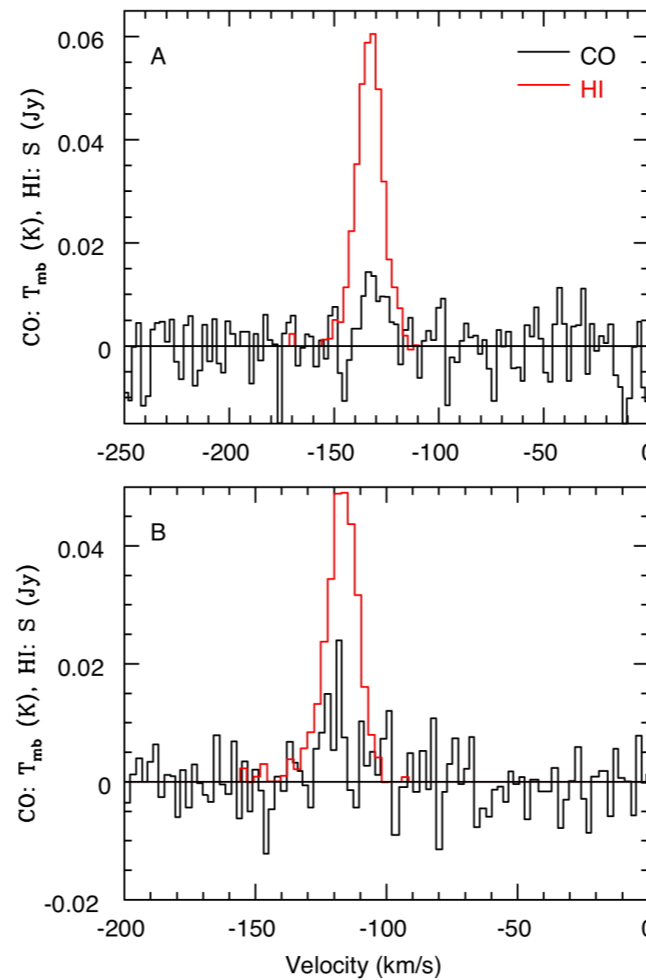
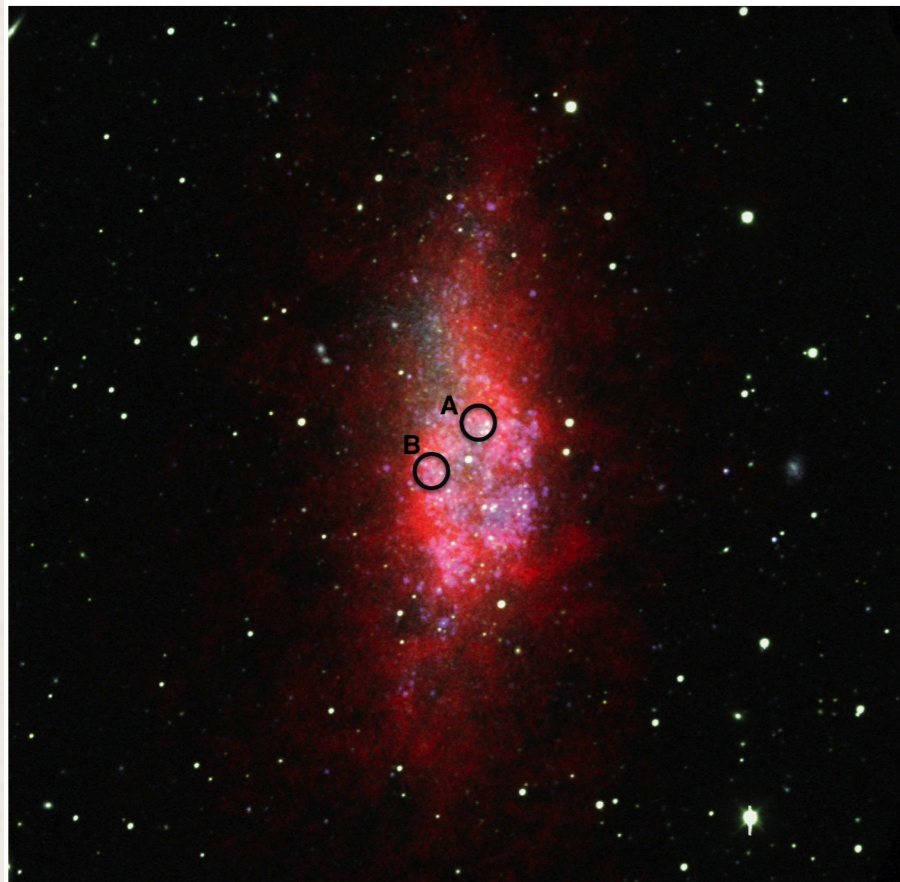
WLM: Wolf-Lundmark-Melotte

- ❖ $D = 985 \pm 33$ kpc
- ❖ $M_* = 1.6 \times 10^7 M_\odot$
- ❖ $M_{\text{HI}} = 7.1 \times 10^7 M_\odot$
- ❖ $V_{\text{rot}} = \sim 36 \text{ km s}^{-1}$
- ❖ $12 + \log(\text{O}/\text{H}) = 7.8$ (SMC: 8.0)
- ❖ $\text{SFR} = 0.006 M_\odot \text{ yr}^{-1}$
- ❖ $s\text{SFR}(\text{WLM}) = 12 \times s\text{SFR}(\text{MW})$

WLM



APEX CO($J=3-2$) detection



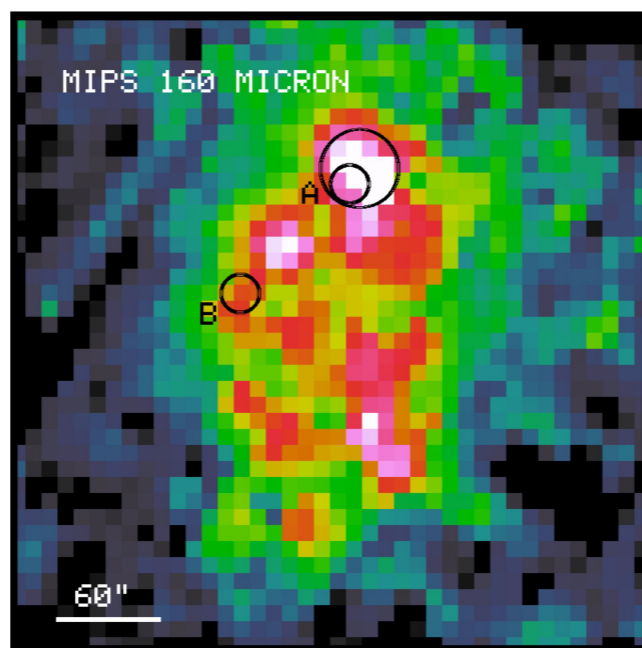
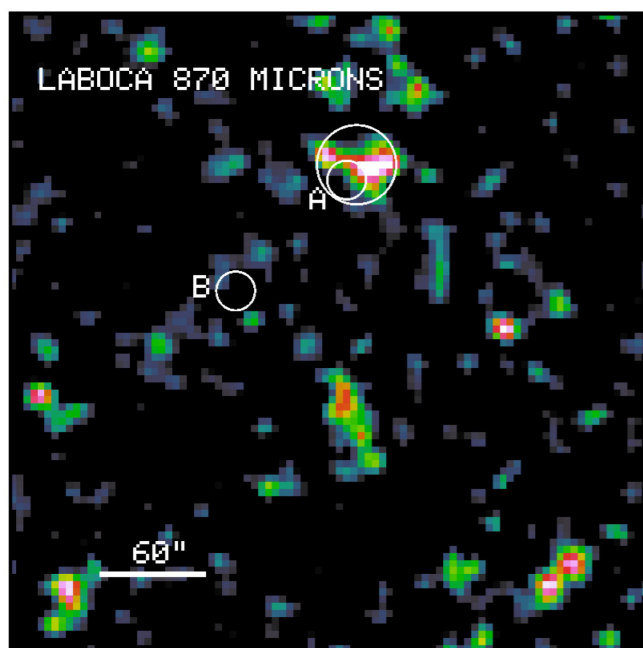
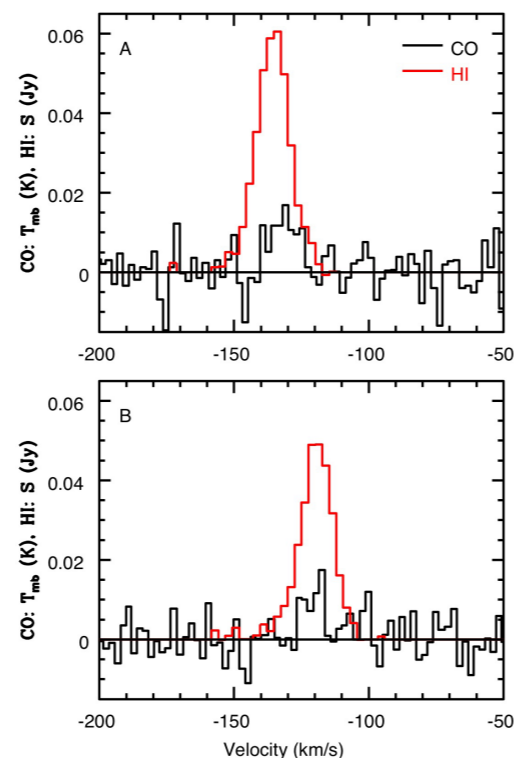
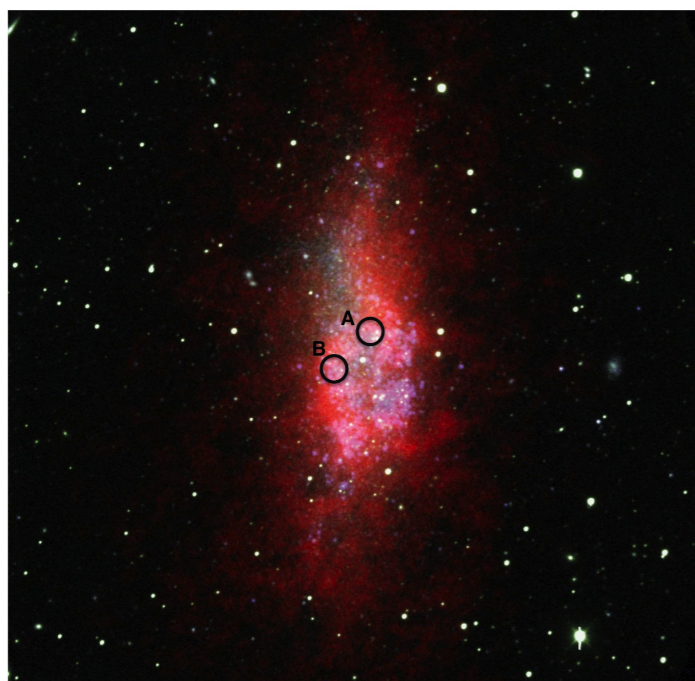
CO ($J=3-2$) detected at two locations in WLM

18" beam

5σ detections

velocity agrees with HI

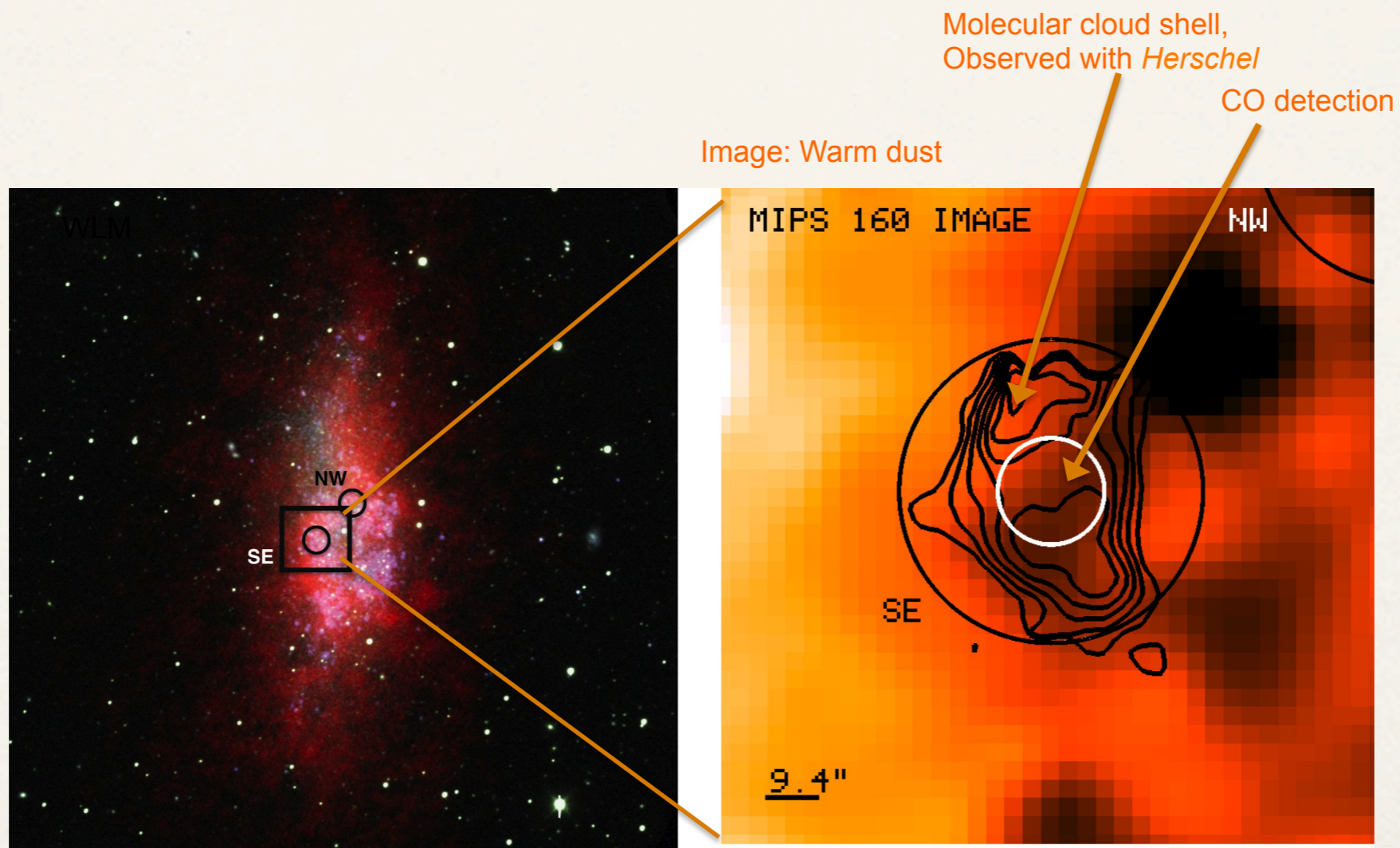
LABOCA cold dust in WLM



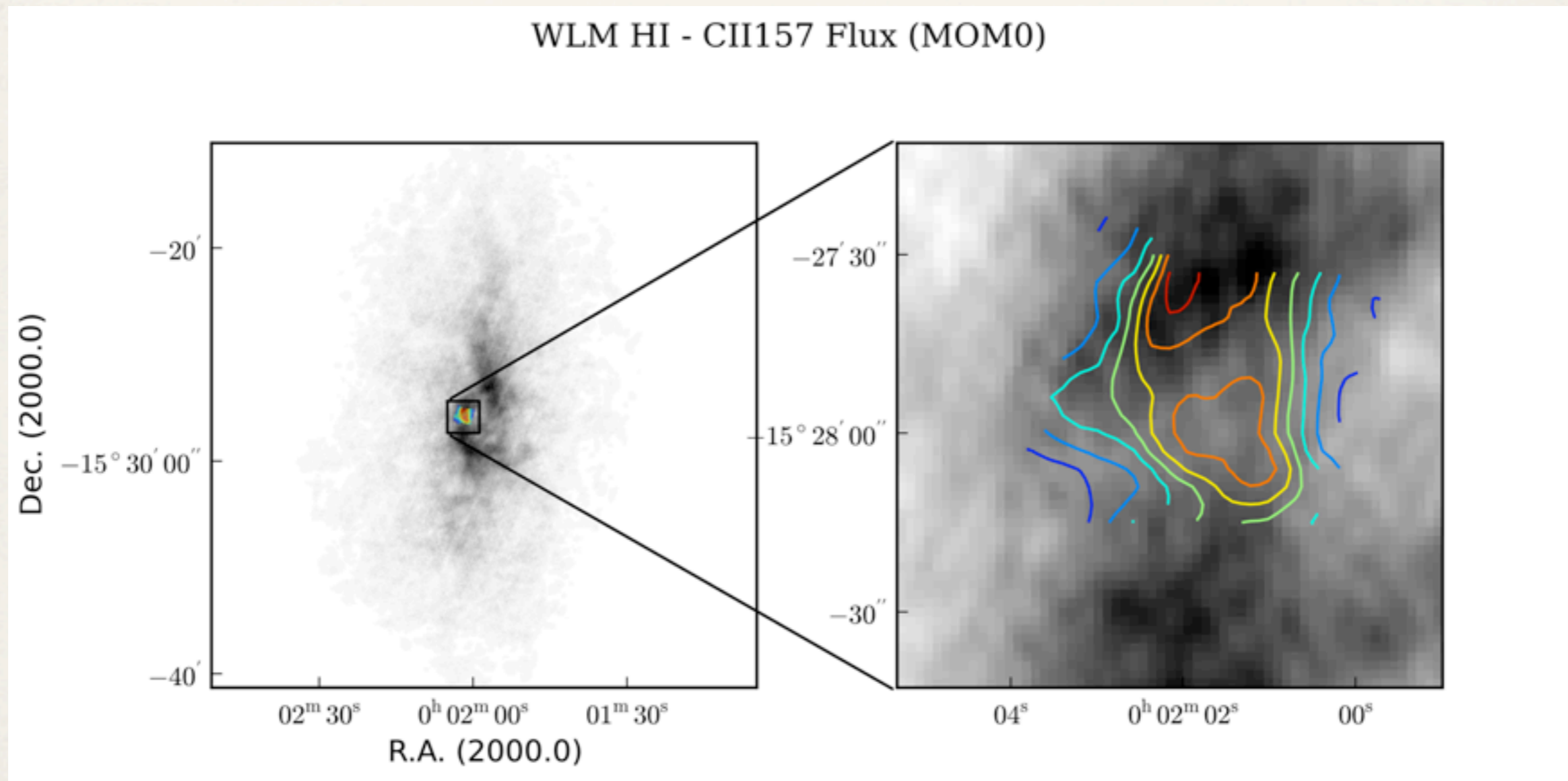
Also, cold dust detected near region A, at 870 μm with LABOCA on APEX

LABOCA detection coincides with *Spitzer* 160 μm

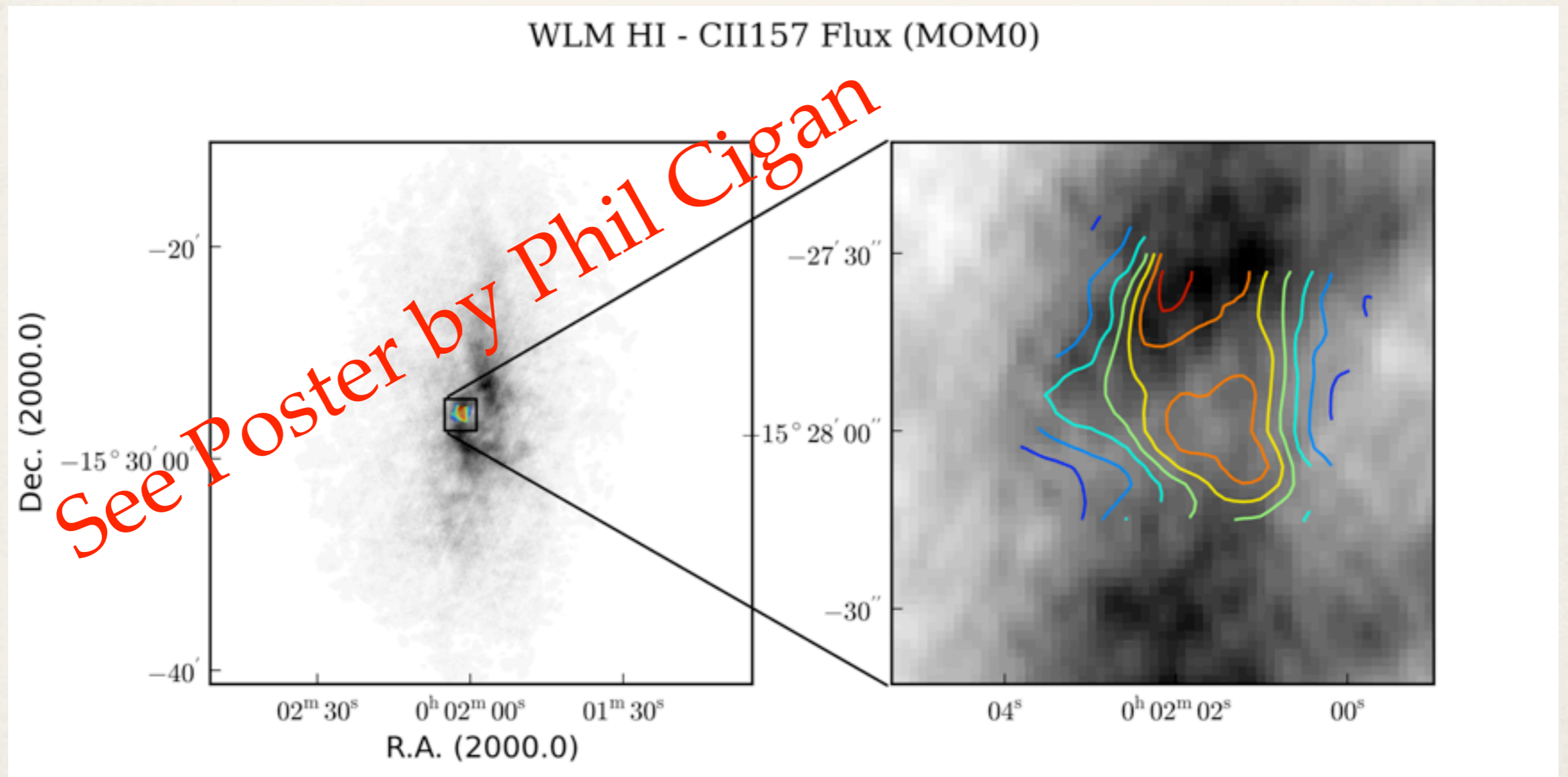
APEX CO($J=3-2$) detection



Herschel PACS [CII] in WLM



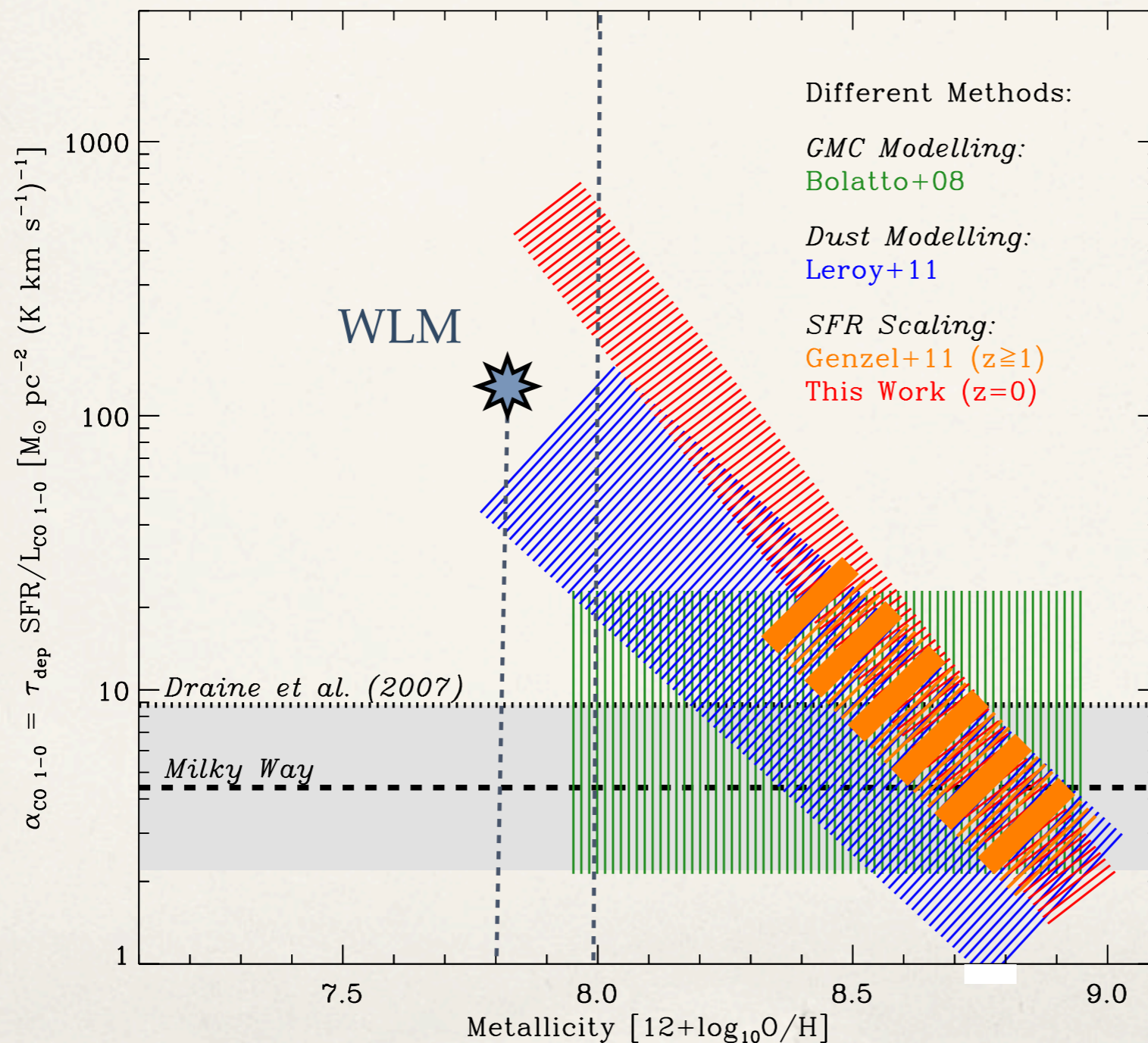
Herschel PACS [CII] in WLM



GMCs in WLM

- ❖ use the MIPS and LABOCA to calculate the dust mass
- ❖ convert the dust mass to a total (HI+H₂) gas mass; we assume that the DGR continues to scale linearly with metallicity, so GDR = 1100 (assumed; MW value of ~145 scaled by [O/H])
- ❖ subtract the observed HI mass; this leaves the H₂ mass
- ❖ GMC mass: $1.8 \pm 0.8 \times 10^5 M_{\odot}$ and $1.2 \pm 0.6 \times 10^5 M_{\odot}$
- ❖ this leads to a mass conversion factor $\alpha_{\text{CO}} = 124 \pm 60 M_{\odot} \text{ pc}^{-2} / (\text{K km s}^{-1})$ or $\sim 30 \times \text{MW value}$ (X_{CO} -factor: $5.8 \pm 2.8 \times 10^{21} \text{ cm}^{-2} / (\text{K km s}^{-1})$)

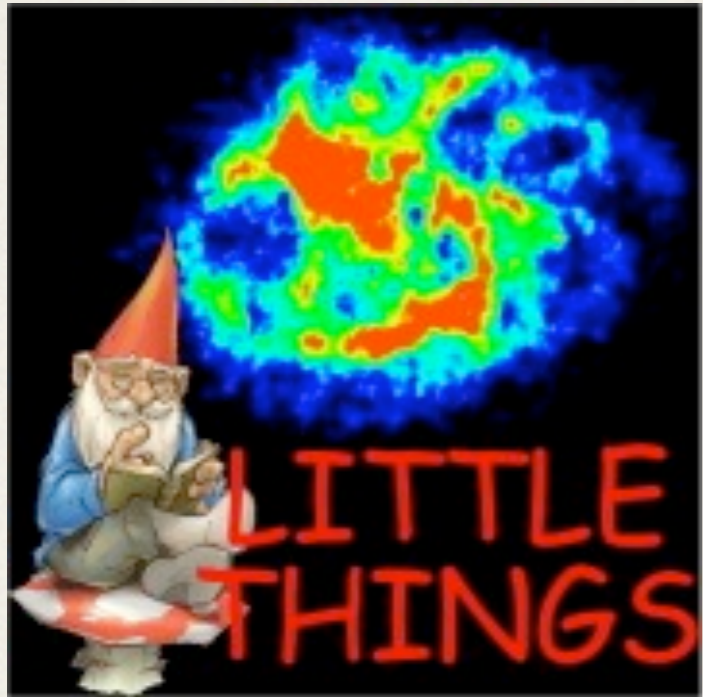
Conversion factor versus metallicity



Schruba et al. 2012,
AJ, 143, 38

Summary

- ❖ LITTLE THINGS is in great shape...watch this space!
- ❖ We broke in WLM ($12+\log(\text{O}/\text{H}) = 7.8$) the low-metallicity limit for a CO detection
- ❖ $\alpha_{\text{CO}} = 124 \pm 60 \text{ M}_{\odot} \text{ pc}^{-2} / (\text{K km s}^{-1})$ or $\sim 30 \times \text{MW value}$
- ❖ GDR = 1100 (assumed; MW value scaled by $[\text{O}/\text{H}]$)
- ❖ GMC mass: $1.8 \pm 0.8 \times 10^5 \text{ M}_{\odot}$ and $1.2 \pm 0.6 \times 10^5 \text{ M}_{\odot}$
- ❖ SFR per molecule in WLM \sim SFR in MW (SFE $\sim 1.5 - 6.7 \text{ Gyr}$)



The End